Molecular Neurobiology (2019) 56:2495–2507
https://doi.org/10.1007/s12035-018-1261-z

Genetic Deletion of Soluble Epoxide Hydroxylase Causes Anxiety-Like Behaviors in Mice

Hsueh-Te Lee[1] · Kuan-I Lee[2] · Hui-Ching Lin[2] · Tzong-Shyuan Lee[3]

Received: 25 May 2018 / Accepted: 17 July 2018 / Published online: 23 July 2018

Abstract

Soluble epoxide hydrolase (sEH), an enzyme with COOH-terminal hydrolase and NH_2-terminal lipid phosphatase activities, is expressed in regions of the brain such as the cortex, white matter, hippocampus, substantia nigra, and striatum. sEH is involved in the regulation of cerebrovascular and neuronal function upon pathological insults. However, the physiological significance of sEH and its underlying mechanism in modulating brain function are not fully understood. In this study, we investigated the role of sEH in anxiety and potential underlying mechanisms in mice. Western blot for protein phosphorylation and expression was performed. Immunohistochemical analyses and Nissl and Golgi staining were performed for histological examination. Mouse behaviors were evaluated by open field activity, elevated plus maze, classical fear conditioning, social preference test, and Morris water maze. Our results demonstrated that the expression of sEH was upregulated during postnatal development in wild-type (WT) mice. Genetic deletion of sEH ($sEH^{-/-}$) in mice resulted in anxiety-like behavior and disrupted social preference. Increased olfactory bulb (OB) size and altered integrity of neurites were observed in $sEH^{-/-}$ mice. In addition, ablation of sEH in mice decreased protein expression of tyrosine hydroxylase and reduced dopamine production in the brain. Moreover, the level of phosphorylated calmodulin kinase II (CaMKII) and glycogen synthase kinase 3 α/β (GSK3α/β) was higher in $sEH^{-/-}$ mice than in WT mice. Collectively, these findings suggest that sEH is a key player in neurite outgrowth of neurons, OB development in the brain, and the development of anxiety-like behavior, by regulating the CaMKII-GSK3α/β signaling pathway.

Keywords sEH · Anxiety · Olfactory bulb · Dopamine · CaMKII · GSK3α/β

Introduction

Soluble epoxide hydrolase (sEH), an enzyme with COOH-terminal hydrolase (EH) and NH_2-terminal lipid phosphatase (PT) activities, is expressed in various mammalian tissues, including the heart, kidney, and central nervous system (CNS) [1–3]. sEH is detectable in vascular cells, astrocytes, and neurons in regions of the brain such as the cortex, white matter (WM), hippocampus, substantia nigra, and striatum [4–6]. The roles of sEH in the metabolism of epoxyeicosatrienoic acids and in the pathogenesis of hypertension and inflammatory diseases have been well defined [7, 8]. Recently, epidemiological studies indicate that genetic variation in sEH is associated with an increased risk of ischemic stroke [9, 10]. Additionally, inhibition of sEH hydrolase activity confers protection from ischemia-induced brain injury in experimental rodents [5, 6, 10–14], suggesting that sEH is a crucial regulator in cerebrovascular and neuronal function upon pathological insults [5, 6, 9, 14, 15]. On the basis of these findings, sEH may be a novel therapeutic target for the treatment of human neurological diseases. However, the involvement of sEH in neuropsychiatric disorders such as anxiety has yet to be investigated.

Anxiety, a common psychiatric disorder, is characterized by excessive rumination, worrying, uneasiness, apprehension, and fear about uncertainties either based on real or imagined events [16, 17]. The etiology and exact molecular mechanisms underlying anxiety remain unclear.

Electronic supplementary material The online version of this article (https://doi.org/10.1007/s12035-018-1261-z) contains supplementary material, which is available to authorized users.

✉ Tzong-Shyuan Lee
ntutslee@ntu.edu.tw

[1] Institute of Anatomy and Cell Biology, National Yang-Ming University, Taipei, Taiwan

[2] Institute and Department of Physiology, National Yang-Ming University, Taipei, Taiwan

[3] Graduate Institute and Department of Physiology, College of Medicine, National Taiwan University, Taipei 10051, Taiwan

Emerging evidence suggests that the hippocampus-prefrontal cortex-amygdala pathway plays an important role in anxiety disorder [18]. Moreover, the dopaminergic pathway negatively regulates the hippocampus-prefrontal cortex-amygdala pathway [19]. Dopamine is predominantly synthesized in neurons of the dopaminergic pathways, mainly in the substantia nigra and ventral tegmental area, and transmitted to their synaptic destinations including the striatum, hippocampus, prefrontal cortex, and amygdala via projecting axons [19, 20]. The olfactory bulb (OB) is an important neural structure in olfaction, which sends olfactory signals to the amygdala and hippocampus for further processing in emotion, memory, and learning [21, 22]. Many psychiatric and neurological disorders are associated with abnormalities in OB function [21]. Loss of function of the OB by bulbectomy or genetic manipulation causes anxiety-like behavior in mice, suggesting a critical role of OB in anxiety disorders [22]. Mechanistically, dysregulation of calmodulin kinase II (CaMKII) phosphorylation and glycogen synthase kinase 3α/β (GSK3α/β) signaling in the brain plays a critical role in anxiety-like behavior [23–26]. Nevertheless, information on the pathophysiologic role of sEH and its underlying mechanism in the development of anxiety is limited.

To address whether sEH participates in the development of anxiety, this study adopted several approaches. First, we delineated the effect of genetic disruption of sEH on behaviors in mice. Second, we investigated the effect of genetic deletion of sEH on brain structure. Third, we explored the potential molecular mechanisms underlying sEH ablation-induced behavioral alterations. We found that sEH-deficient mice exhibited anxiety-like behaviors accompanied with increased CaMKII and GSK-3α/β phosphorylation, as well as lower levels of dopamine in the brain compared to those in wild-type (WT) mice. These findings suggest that sEH may play a crucial role in the regulation of anxiety.

Methods

Reagents

Antibodies for GSK3α/β, serine-phosphorylated GSK3α/β, tyrosine-phosphorylated GSK3α/β, sEH, tyrosine hydroxylase (TH), dopamine transporter (DAT), serotonin transporter (ST), tryptophan hydroxylase (TPH), CaMKII, proliferating cell nuclear antigen (PCNA), and β3-tubulin were obtained from Santa Cruz Biotechnology (Santa Cruz, CA, USA). Rabbit anti-goat FITC-conjugated antibody, rabbit anti-mouse rhodamine-conjugated antibody, mouse antibody for α-tubulin, bovine serum albumin (BSA), phosphatase inhibitor cocktails, 12-(3-adamantan-1-yl-ureido)-dodecanoic acid (AUDA), and Ebselen were obtained from Sigma-Aldrich (St. Louis, MO, USA). Rabbit antibodies for phosphorylated CaMKII and CaMKII were obtained from Cell Signaling Technology (Danvers, MA, USA). Dopamine ELISA assay kit was obtained from Abnova (Taoyuan, Taiwan). GSK3α/β activity ELISA assay was obtained from Novus Biologicals (Littleton, CO, USA). 12-(3-Adamantan-1-yl-ureido)-dodecanoic acid (AUDA) was synthesized as described [27].

Mice

The experiments conformed to the Guide for the Care and Use of Laboratory Animals (Institute of Laboratory Animal Resources, eighth edition, 2011). All animal experiments were approved by the Animal Care and Utilization Committee of National Yang-Ming University. WT C57BL/6 mice were purchased from the National Laboratory Animal Center, Ministry of Science and Technology (Taipei, Taiwan). $Ephx2^{tm1/Gon2/J}$ ($sEH^{-/-}$) mice on a C57BL/6 background were purchased from Jackson Laboratory (Bar Harbor, ME, USA). $sEH^{-/-}$ mice were backcrossed to C57BL/6J for at least 10 generations. Male WT mice received AUDA (20 mg/kg), ebselen (10 mg/kg), or saline (vehicle control) daily by gastric gavage for 7 days. At the end of experimentation, mice were subjected to behavioral testing and were then euthanized with CO_2. Brains were harvested for histopathology or stored at − 80 °C for western blot analysis and ELISA assays.

Immunoprecipitation Assay and Western Blot Analysis

Frozen lysates were homogenized and lysed in immunoprecipitation lysis buffer (50 mmol/L Tris pH 7.5, 5 mmol/L EDTA, 300 mmol/L NaCl, 1% Triton X-100, 1 mmol/L phenylmethylsulfonyl fluoride, 10 μg/mL leupeptin, 10 μg/mL aprotinin, tyrosine phosphatase cocktail I, and serine/threonine phosphatase cocktail II). Aliquots (1000 μg) of tissue lysates were incubated with specific primary antibodies overnight at 4 °C and then with protein A/G-Sepharose for 2 h. Immune complexes were collected by centrifugation, washed three times with cold phosphate-buffered saline (PBS), and then eluted in sodium dodecyl sulfate (SDS) lysis buffer (1% Triton, 0.1% SDS, 0.2% sodium azide, 0.5% sodium deoxycholate, 10 μg/mL leupeptin, and 10 μg/mL aprotinin). Eluted protein samples were separated on SDS-PAGE and then samples were transferred to membrane and immunoblotted (IB) with primary antibodies, then horseradish peroxidase-conjugated secondary antibodies. Bands were revealed by use of an enzyme-linked chemiluminescence detection kit (PerkimElmer, Waltham, MA, USA), and density was quantified by use of Imagequant 5.2 (Healthcare Bio-Sciences, PA, USA).

Histology and Staining

Mouse brain tissue was fixed with 4% paraformaldehyde, embedded in paraffin and serially sectioned at 15 μm. The brain sections underwent Nissl staining by incubating sections with 0.1% crystal violet in PBS for 30 min. For Golgi staining, brain samples were placed into 3% potassium dichromate in 4% paraformaldehyde for 2 days in the dark, followed by 2% silver nitrate in distilled deionized water for an additional 2 days. After staining, brain samples were embedded in paraffin and then sectioned at 20 μm.

Immunofluorescence Staining

Five brain sections were randomly selected from each mouse and then subjected to immunofluorescence staining. The deparaffinized sections were incubated with retrieval buffer for 10 min, blocked with 2% BSA for 60 min, and incubated with primary antibody overnight at 4 °C, and then FITC- or rhodamine-conjugated secondary antibody for 1 h at 37 °C. Antigenic sites were visualized under a Nikon TE2000-U microscope (Tokyo) with QCapture Pro 6.0 software (QImaging, BC, Canada). The fluorescence intensity of sections was quantified by use of ImageJ software (http://rsbweb.nih.gov/ij/download.html).

TUNEL Staining

DNA fragmentation was determined by the TdT-mediated dUTP nick end labeling (TUNEL) method (Boehringer Mannheim). Briefly, after incubation with proteinase K (20 μg/ml) for 20 min, brain sections were incubated with FITC-dUTP and terminal deoxynucleotidyl transferase, which catalyzes the incorporation of FITC-dUTP to the 3′-OH ends of DNA fragments. Images were viewed under a TE2000-U fluorescence microscope and quantified with the use of QCapture Pro 6.0.

Open Field Activity

The locomotor activity of mice was assessed in a cage (length × width × height: 28.5 × 28.5 × 30 cm). Mice were placed in the center of the cage and allowed to explore the open field for 5 min. The behavior was recorded by video. The movement distance, percentage of resting time in the zone, and trajectory were calculated for each mouse using Smart v3.0 software with the Panlab Harvard apparatus (Cornellà, Barcelona, Spain). The floor and internal walls were cleaned with ethanol between each trial.

Elevated Plus Maze

The elevated plus maze (EPM) was used for investigating anxiety-like behavior in mice. The maze consisted of two open arms and two enclosed arms (30 × 6 cm with 20-cm high walls in black acrylic). The maze was elevated 50 cm above the floor. Mice were placed in the center square facing an open arm and allowed to explore the maze for 10 min. Time spent in the open arms, closed arms, or central area was recorded using Smart v3.0. The floor and internal walls were cleaned with ethanol between each trial.

Classical Fear Conditioning

The experiments were performed using a computerized fear conditioning system purchased from Coulbourn Instruments (San Diego, CA, USA). The system consisted of a shock and a tone generator. Training took place in an apparatus consisting of a box (22 × 22 × 30 cm) with a simple gray interior and a 12-V light attached to the ceiling. At the beginning of experiments, each mouse was exposed to the conditioning chamber for 2 min, where the mice were exposed to conditioning stimuli (CS), a tone (2000 Hz, 80 dB) for 20 s and received foot shock (FS) at 1.5 mA for 3 s. This conditioning training was repeated three times with an inter-trial delay of 30 s. Finally, analysis of the freezing behavior ratio while exposed to the tone (CS) was performed as a measure of learning activity. The freezing response was defined as the absolute lack of movement (excluding respiratory movements), monitored by an ultra-red ray detector and analyzed by a computer. On day 2, the conditioned mice were re-exposed to CS training three times for duration of 20 s each. The percentage of freezing responses was scored.

Social Preference Test

The protocol for the social interaction test was modified from Jamain S. et al. [28]. Social interaction between the isolated mouse and a visitor was recorded. The social box area was 60 × 30 × 30 cm. The social preference assay consisted of two phases. In the habituation phase (phase 1), a mouse was placed in the cage and allowed to freely explore the box for 5 min. In the social preference phase (phase 2), a stranger or familiar mouse was placed into a small chamber and allowed to sniff. The exploration time spent in the mouse area and the empty area was immediately recorded for 10 min. The individual path length, trajectory, and time spend in different zones were analyzed using Smart v3.0. The proportion of time in the target zone was calculated by the time in the zone with the stranger or familiar mouse/time in the two zones × 100.

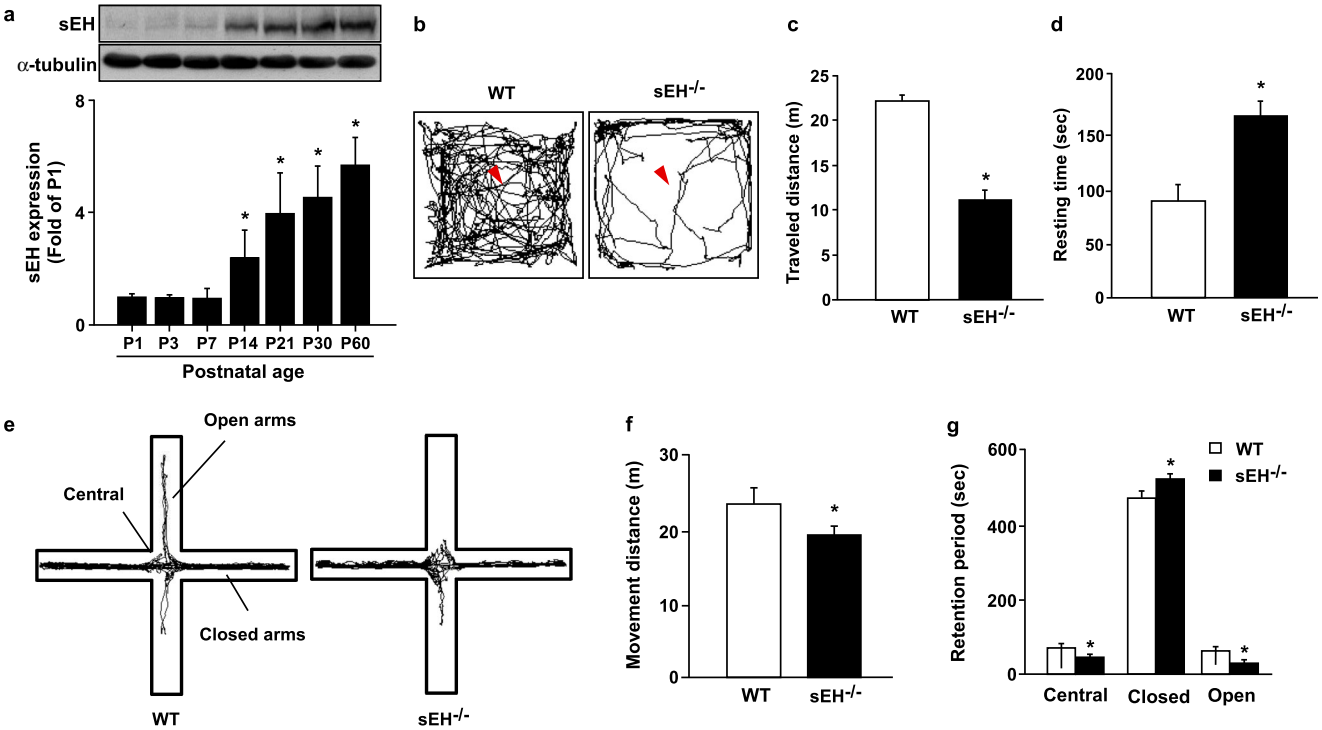

Fig. 1 Genetic deletion of sEH increases anxiety-like behavior in mice. **a** Brain lysates were collected from WT mice ($n = 5$ in each group) at indicated times. Western blotting analysis of sEH and α-tubulin. **b** Representative activity traces from WT mice and $sEH^{-/-}$ mice in the open field test. **c**, **d** Total distance traveled and resting time of WT mice and $sEH^{-/-}$ mice were analyzed in the entire open field activity test ($n = 10$ in each group). **e** Representative activity traces in the elevated plus maze (EPM) test of WT mice and $sEH^{-/-}$ mice. **f**, **g** Total distance traveled and times spent by WT and $sEH^{-/-}$ mice in the central, closed, and open arms of an elevated plus maze ($n = 10$ in each group). Data are presented as mean ± SEM. In **a**, $^*p < 0.05$ vs. P1 group. In **c**, **d**, **f**, and **g**, $^*p < 0.05$ vs. WT mice

Morris Water Maze

The Morris water maze (MWM) was performed for evaluating hippocampus-dependent spatial learning and memory in mice. A large circular tank (0.8-m diameter, 0.4-m depth) was filled with water (25 ± 1 °C, 20 cm depth), and the escape platform (8 × 4 cm) was submerged 1 cm below the surface. Each section was monitored by a video 9system. The escape latency and trajectory of swimming were recorded for each mouse. The hidden platform was located at the center of one of the four quadrants in the tank. The location of the platform was fixed throughout testing. Mice had to navigate using extra-maze cues that were placed on the walls of the maze. From day 1 to 4, mice underwent three trials with an inter-trial interval of 5 min. The mice were placed into the tank facing the side wall randomly at one of four start locations and allowed to swim until they found the platform or for a maximum of 120 s. Each mouse that failed to find the platform within 120 s was guided to the platform. The animal then remained on the platform for 20 s before being removed from the pool. The day after the hidden platform training, a probe trial was conducted to determine whether mice used a spatial strategy to find the platform. On day 5, the platform was removed from the pool and the mouse was allowed to swim freely for 120 s. The proportion of time spent in each quadrant of the pool and the number of times the mice crossed the former position of the hidden platform were recorded.

Measurement of Dopamine

The concentrations of dopamine in brain were measured using an ELISA kit according to the manufacturer's instructions. The brains were grinded in a mortar and lysed in SDS lysis buffer (1% Triton X-100, 0.1% SDS, 0.1% sodium deoxycholate, 1 μg/ml leupeptin, 10 μg/ml aprotinin, 1 mM phenylmethylsulfonyl fluoride) on ice for 30 min and then centrifuged at 12000 rpm for 5 min to collect the supernatant. The diluted brain lysates were added to the microplates, and then each well sequentially added assay diluent, mouse dopamine conjugate, substrate solution, and stop solution. The microplates were read at 450 nm by an ELISA reader (Infinite 200 PRO). The concentrations were calculated by comparison with the standard curve.

Measurement of GSK3α/β Activity

The activity of GSK3α/β in fresh brain lysates was measured by GSK3α/β activity ELISA assay according to the manufacturer's instructions.

Statistical Analysis

Results are presented as mean ± standard deviation (SD). The Mann- Whitney *U* test was used to compare two independent groups. Kruskal-Wallis followed by Bonferroni post hoc analyses were used to account for multiple testing. SPSS v19.0 (SPSS Inc., Chicago, IL, USA) was used for analysis. Differences were considered statistically significant if $P < 0.05$.

Results

Genetic Ablation of sEH Induces Anxiety-Like Behaviors in Mice

sEH protein expression in the brain was increased in a postnatal development-dependent manner (Fig. 1a). Loss of function of sEH in mice decreased locomotive activity in the open field test (Fig. 1b–d). Compared to WT mice, sEH null mice exhibited anxiety-like behaviors as evidenced by increased time spent in the closed arm but decreased retention time in the central and open arms, with a slight decrease in locomotion in the EPM test (Fig. 1e–g). These results suggest that sEH may play a role in anxiety-like behaviors.

Genetic Deletion of sEH Enhances Hippocampus-Dependent Fear-Related Learning, Amygdala-Dependent Fear-Related Memory, and Social Recognition Behavior in Mice

The fear conditioning paradigm we used is schematized in Fig. 2a. In trial 3 on day 1, $sEH^{-/-}$ mice showed an enhanced learning trajectory as evidenced by higher freezing rates than those in WT mice (Fig. 2b). On day 2, the freezing rate of $sEH^{-/-}$ mice following cue delivery was significantly higher than that in WT mice with all three cues (Fig. 2c). However, the results of the MWM test showed that loss of function of sEH did not interfere with hippocampus-dependent learning and memory (Fig. S1). In the social preference test, there was no difference in time spent by $sEH^{-/-}$ mice interacting with stranger mice compared to that of WT mice (Fig. 3a, b). However, the difference in time spent by $sEH^{-/-}$ mice interacting with familiar mice was significantly greater than that of WT mice (Fig. 3c, d). These findings suggest that sEH may be involved in regulating hippocampus-dependent fear-

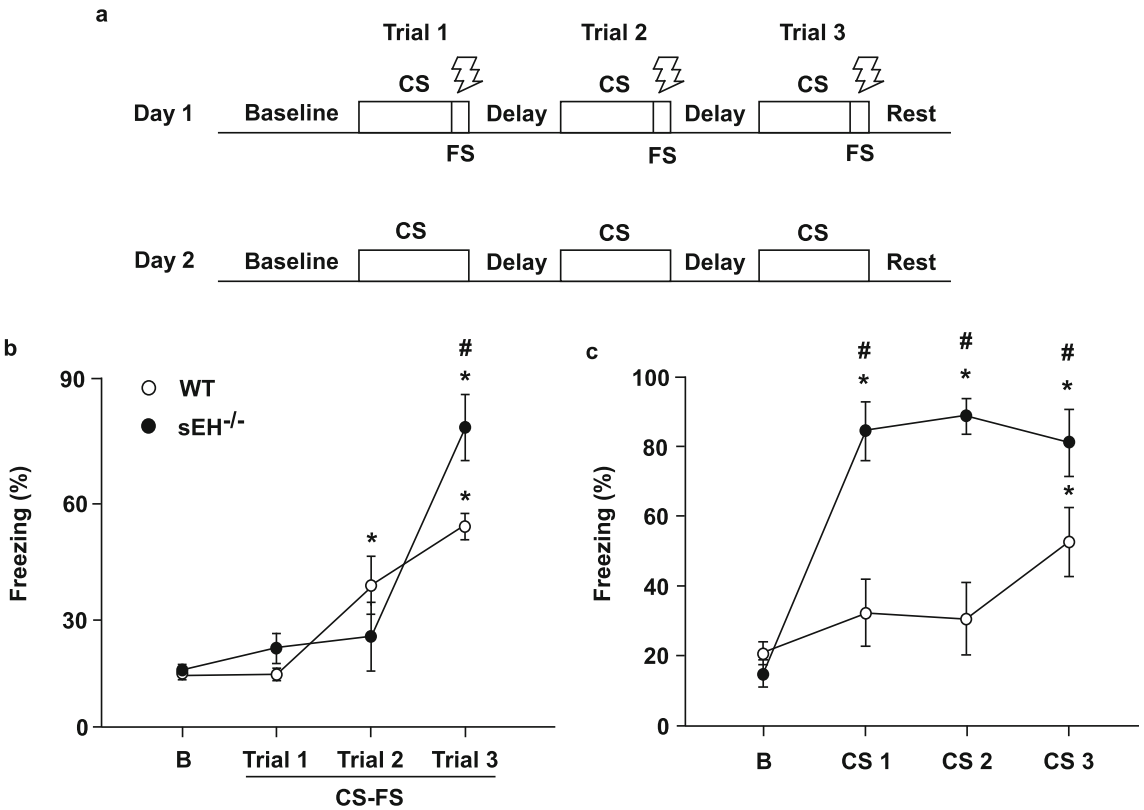

Fig. 2 Loss of sEH enhances the ability of hippocampus-dependent fear-related learning and amygdala-dependent fear-related memory in mice. **a** The experimental design for the fear conditioning test. **b** The freezing behavior changes after a foot shock (FS) were used to assess hippocampus-dependent learning on day 1. **c** Freezing behavior after conditioning stimuli (CS) on day 2 was used to assess amygdala-dependent memory. Data are presented as mean ± SEM from 10 mice in each group. *$p < 0.05$ vs. baseline; #$p < 0.05$ vs. WT mice with corresponding trial/stimulus. B baseline

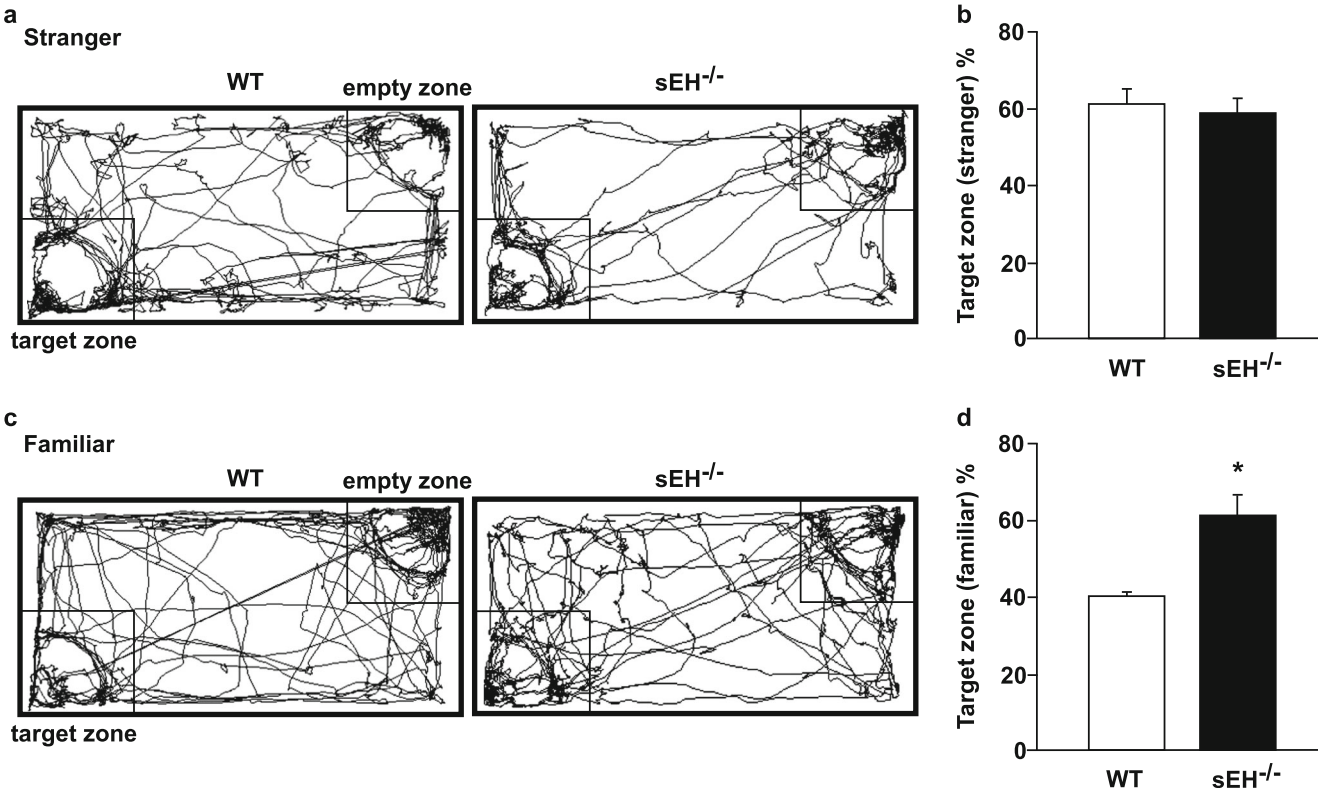

Fig. 3 sEH$^{-/-}$ mice exhibit enhanced social discrimination to familiar mice as interactive partners. **a**, **c** Representative running tracks and **b**, **d** social preference of WT mice and sEH$^{-/-}$ mice contacting the stranger or familiar mouse, respectively. Data are presented as mean ± SEM from 10 mice in each group. *$p < 0.05$ vs. WT mice

related learning, amygdala-dependent fear-related memory, and social recognition in mice.

sEH Deficiency in Mice Presents with OB Malformation and Increased Neurite Integrity

Gross anatomical analysis of the brain demonstrated that sEH$^{-/-}$ mice displayed an increase in OB size compared to that of WT mice (Fig. 4a). The expression of sEH was found in the granular cell layer of OB (GrO) in WT mice (Fig. S2a). Moreover, histological examination demonstrated that sEH$^{-/-}$ mice exhibited an increased area of GrO and olfactory ventricle (OV) compared to that in WT mice (Fig. 4b). We next examined whether dysregulation of cell proliferation and apoptosis contributes to the enlarged size of OB in sEH$^{-/-}$ mice. Compared to WT mice, we observed an increased expression of PCNA, a proliferation marker; but decreased cell apoptosis, in OB of sEH$^{-/-}$ mice (Fig. 4c, d). Additionally, the results of Golgi staining demonstrated that more complex neurites were found in the WM and hippocampus of sEH$^{-/-}$ mice compared to those of WT mice (Fig. 5a, b). Western blot analysis and immunofluorescence staining further revealed that the level of β3-tubulin protein in the brain was higher in sEH$^{-/-}$ mice compared to WT mice (Fig. 5c, d). The increased neurite integrity and β3-tubulin expression were also observed in the external plexiform layer (EPI) of GrO (Fig. S2b-d). These findings suggest that sEH may play a pivotal role in both OB development and neurite outgrowth.

Genetic Loss of sEH in Mice Leads to Decreased Dopamine Level and TH Protein Expression but Increased Phosphorylation of CaMKII and GSK3α/β

Results from ELISA demonstrated that dopamine concentration in the brain was lower in sEH$^{-/-}$ mice than that in WT mice (Fig. 6a). We then used immunofluorescence staining and western blot analysis to examine the protein level of TH, a key enzyme in dopamine synthesis. Results of immunofluorescence staining revealed that sEH$^{-/-}$ mice displayed lower expression of TH in the striatum and substantia nigra (Fig. 6b). Western blot analysis showed that the protein level of TH, but not DAT, TPH, or ST, was lower in the brains of sEH$^{-/-}$ mice compared to WT mice (Fig. 6c–g).

Next, we examined whether sEH was involved in the regulation of phosphorylation of CaMKII and GSK3α/β in mice. Our results demonstrated that phosphorylation of CaMKII was markedly increased in the brains of sEH$^{-/-}$ mice (Fig. 7a). The phosphorylation of GSK3α at ^{21}Ser and

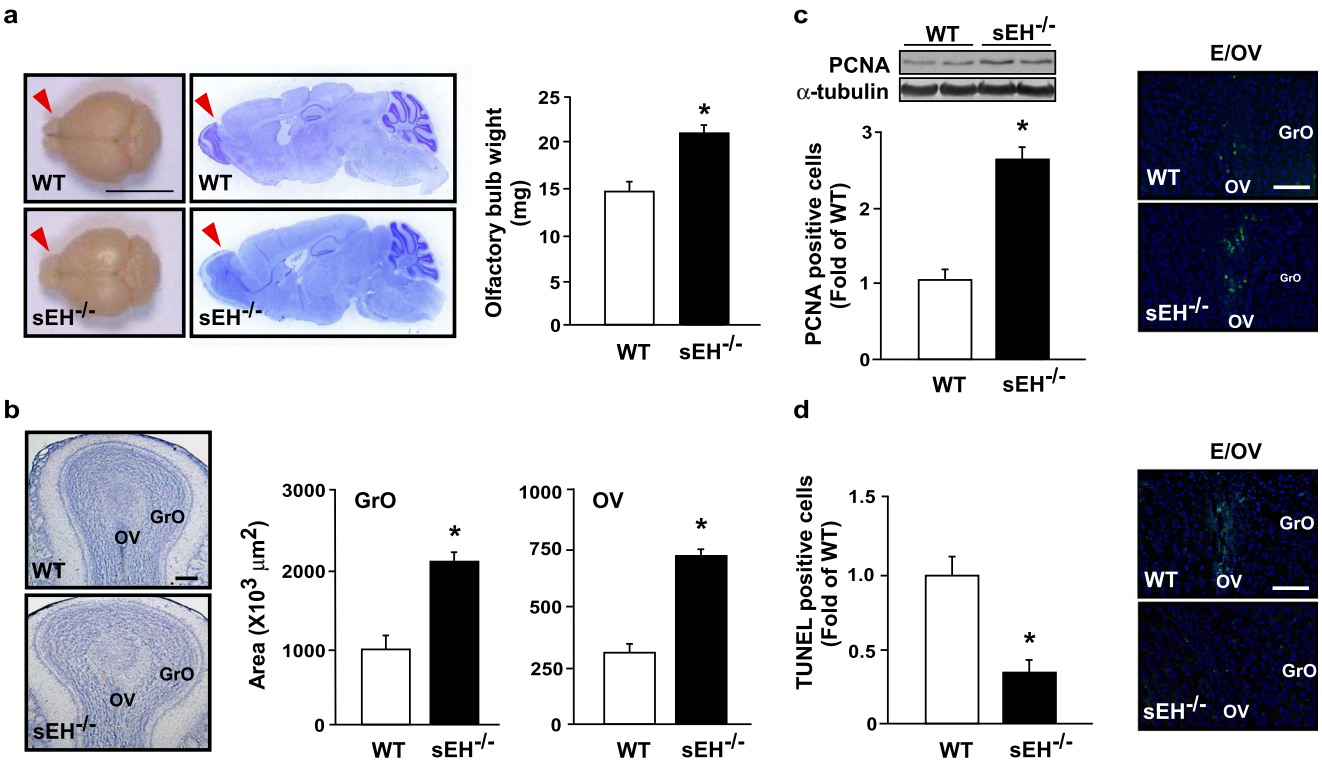

Fig. 4 Macroscopic and microscopic analyses of olfactory bulbs (OB) from WT and sEH$^{-/-}$ mice. **a** Macroscopic view of OB and the corresponding Nissl-stained sagittal sections of mice brains ($n = 10$ in each group). **b** Nissl-stained horizontal sections of OB in mice. The area of the granular cell layer of olfactory bulb (GrO) and olfactory ventricle (OV) were calculated from WT mice and sEH$^{-/-}$ mice ($n = 5$ in each group). **c** Western blotting analysis of PCNA and α-tubulin in OB lysates. Double immunofluorescence staining of PCNA in ependymal/olfactory ventricle (E/OV) of mice ($n = 5$ in each group). **d** TUNEL-positive cells and quantification of WT mice and sEH$^{-/-}$ mice in E/OV ($n = 5$ in each group). In **a**, scale bars = 1 cm. In **b**, **c**, and **d**, scale bars = 100 μm. Data are presented as mean ± SEM. *$p < 0.05$ vs. WT mice

GSK3β at ^{9}Ser was increased in sEH$^{-/-}$ mice (Fig. 7b–d). However, genetic deletion did not change the phosphorylation of GSK3α at ^{279}Tyr or GSK3β at ^{216}Tyr (Fig. 7e, f). Results of ELISA further showed that the activity of GSK3α/β in the brain was decreased in sEH$^{-/-}$ mice (Fig. 7g). Moreover, we observed the formation of sEH-GSK3α/β and sEH-CaMKII complexes as revealed by immunoprecipitation (IP) assay in the brains of WT mice (Fig. 7h). These findings suggest that sEH may be implicated in the regulation of TH expression, dopamine production, and phosphorylation of CaMKII and GSK3α/β.

The PT Activity of sEH Is Involved in Regulating Anxiety-Like Behavior

We further examined which enzymatic activity of sEH participates in the regulation of anxiety-like behavior in mice. WT mice treated with ebselen (a specific inhibitor of PT activity of sEH) or AUDA (a specific inhibitor of EH activity of sEH) did not demonstrate behavioral changes compared to vehicle-treated mice in the open field activity test (Fig. 8a–c). These results suggest that the PT activity of sEH may be response for the dysregulation of anxiety-like behaviors in sEH$^{-/-}$ mice. Collectively, these findings suggest that sEH may regulate anxiety-like behavior (Fig. 9).

Discussion

In the present study, we identified a novel role for sEH in the regulation of anxiety-like behaviors in mice. We demonstrated that the protein expression of sEH in the brain was increased during postnatal development in WT mice. Histologically, the size of the OB in sEH$^{-/-}$ mice was increased, especially in the regions of GrO and OV. This may potentially be due to dysregulation of the balance between cell proliferation and apoptosis. At the cellular level, deletion of sEH in mice altered the neurite structure of neurons in OB and hippocampus. Moreover, increased anxiety-related behaviors and social anxiety were observed in sEH$^{-/-}$ mice as demonstrated in open field activity, EPM, and social preference test. Additionally, sEH$^{-/-}$ mice displayed enhanced hippocampus- and amygdala-dependent brain functions as evidenced by enhanced ability in fear-related learning and memory. Based on biochemical analysis, sEH$^{-/-}$ mice exhibited a lower level of dopamine than that in WT mice, which may be attributed to the downregulation of TH in the brain. Furthermore, ablation

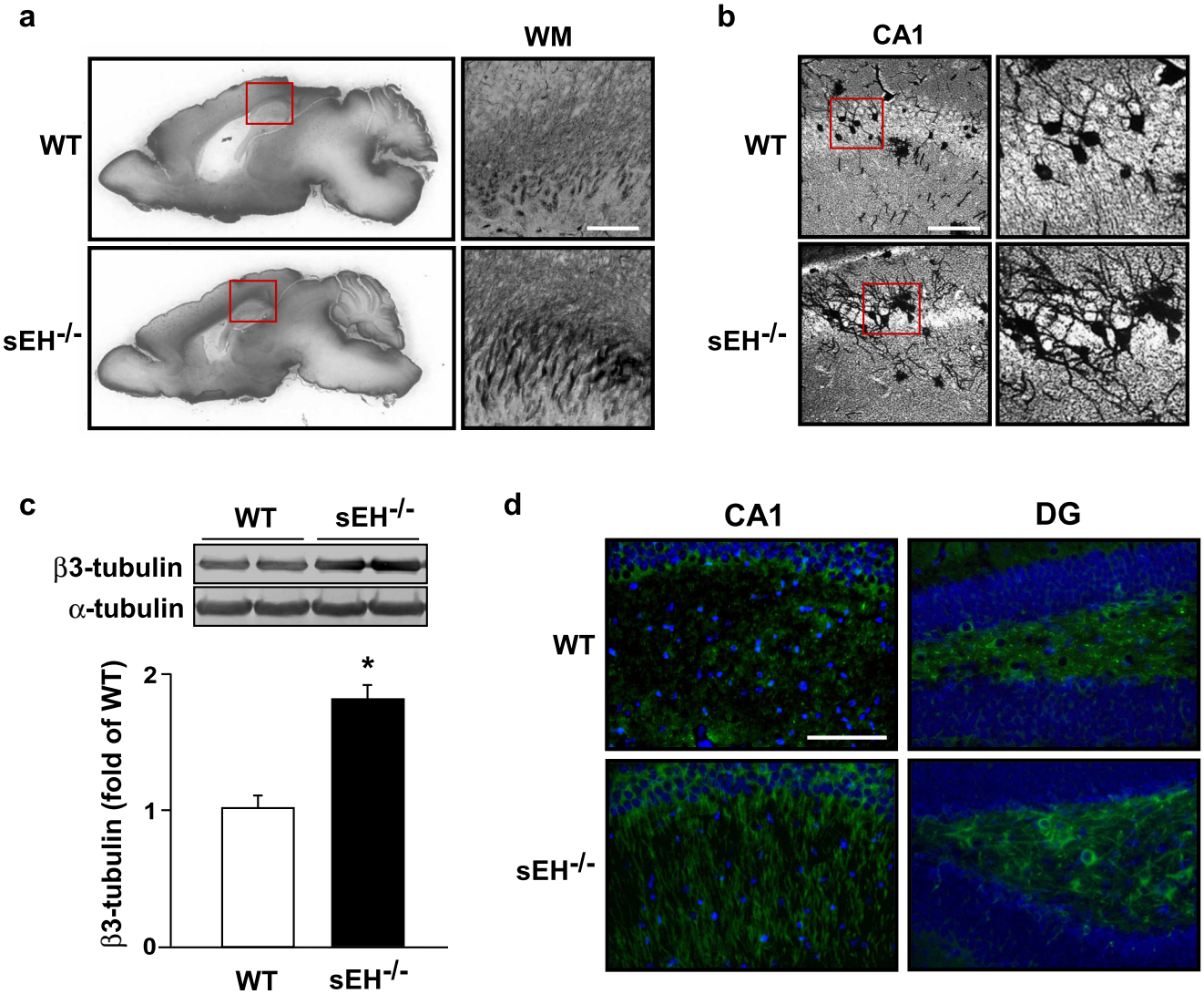

Fig. 5 sEH$^{-/-}$ mice show altered bundle structure in white matter (WM) and neurite morphology of neurons in the hippocampus with increased β3-tubulin expression. **a**, **b** Golgi staining of bundle structure in WM and neurites of pyramidal neurons in CA1 from WT and sEH$^{-/-}$ mice. **c** Western blotting analysis of β3-tubulin and α-tubulin in brain lysates of WT and sEH$^{-/-}$ mice ($n = 5$ in each group). **d** Double-label immunofluorescence of β3-tubulin and DAPI in CA1 region and dentate gyrus (DG) of hippocampus of WT and sEH$^{-/-}$ mice. In **a** and **b**, scale bar = 50 μm. In **c**, scale bar = 100 μm. Data are presented as mean ± SEM. *$p < 0.05$ vs. WT mice

of sEH resulted in hyperphosphorylation of CaMKII and GSK3α/β. Collectively, our study provides new insights into the pivotal role of sEH in regulating the emotional functions of the brain.

The biological significance of sEH in pathological CNS disorders has been documented by previous studies [9–14]. However, most studies have focused on how inhibition of sEH hydrolase activity protects experimental animals from ischemia-induced brain injury [9–14]. Nevertheless, little is known about the physiological role of sEH in the CNS. Past research has elucidated the importance of the OB and neurite structure of neurons in anxiety-like behavior [22, 29–32]. Here, we demonstrated that sEH was expressed in neurons of GrO in OB. Ablation of sEH in mice increased the size of OB and dysregulated the neurite structure of neurons in OB and hippocampus by upregulation of β3-tubulin. In parallel, our cellular and molecular evidence indicated that deficits in sEH markedly increased the area of GrO and OV. Interestingly, we found that deletion of sEH in mice resulted in increased cell proliferation but decreased cell apoptosis in the region of E/OV, which may account for the enlarged GrO and OV in sEH$^{-/-}$ mice. Ample evidence indicates that new neurons generated from stem cells in the subventricular zone migrate toward the OB, where they differentiate into granule and periglomerular cells, after which they integrate into the existing circuitry in adult rodents [33]. Therefore, the normal developmental program in the OB is crucial for

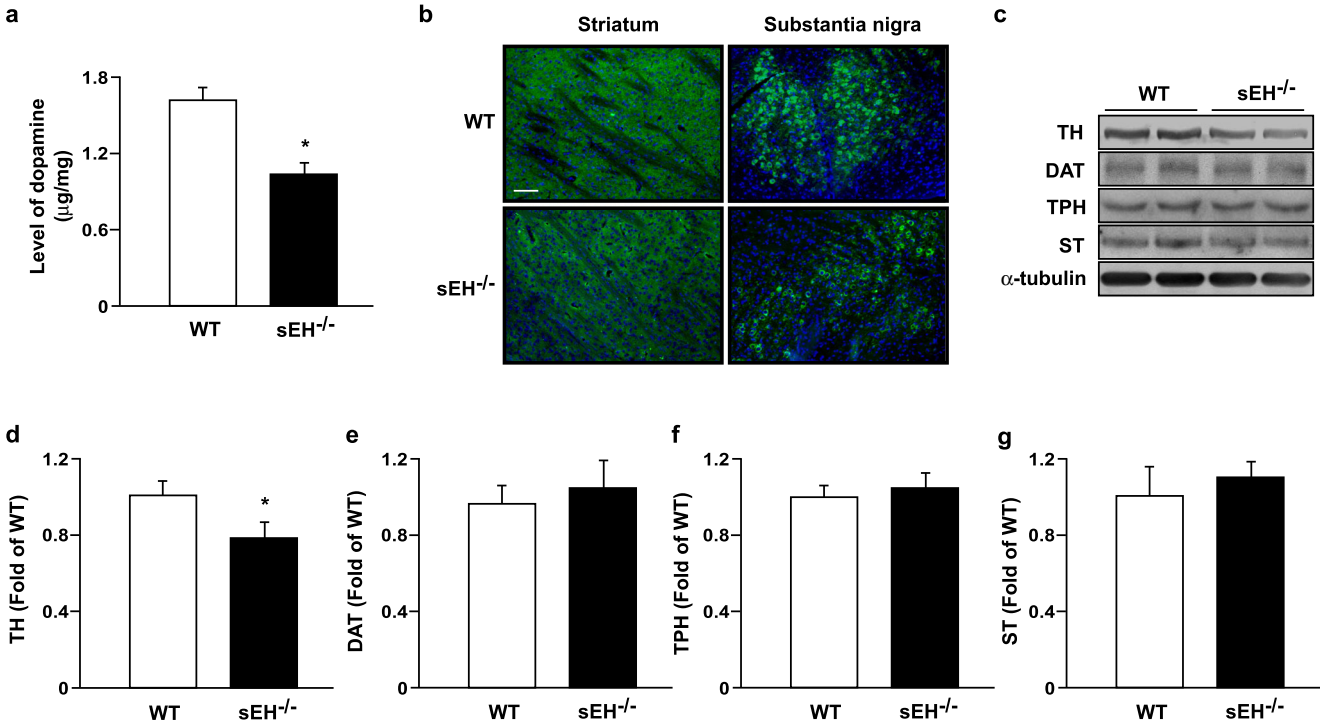

Fig. 6 Protein expression of tyrosine hydroxylase (TH) and dopamine level were decreased in sEH$^{-/-}$ mice. **a** The level of dopamine in brain lysates was measured by ELISA. **b** Immunofluorescence of TH and DAPI in the striatum and substantia nigra of mice. **c** Western blotting analysis of TH, dopamine transporter (DAT), tryptophan hydroxylase (TPH), serotonin transporter (ST), and α-tubulin in brain lysates of WT and sEH$^{-/-}$ mice. **d**–**g** Quantification of the western blotting. Scale bar = 100 μm. Data are presented as mean ± SEM from 5 mice in each group. *$p < 0.05$ vs. WT mice

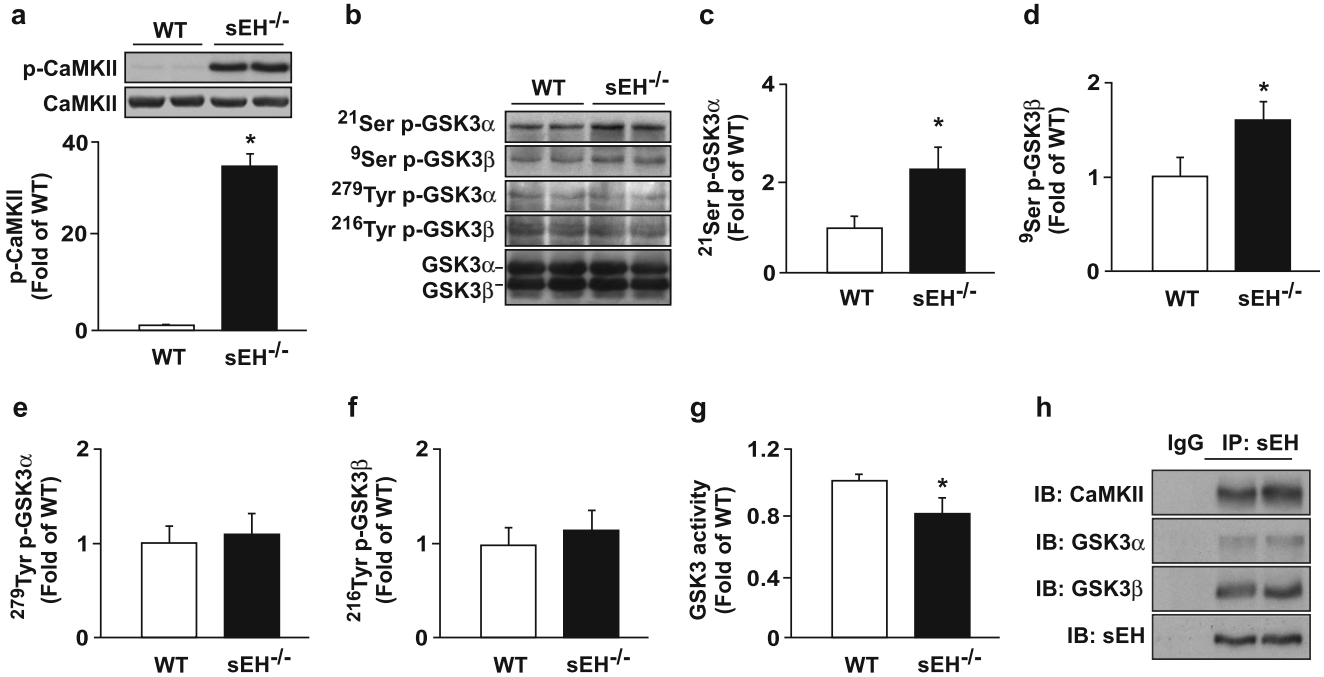

Fig. 7 sEH plays a crucial role in the regulation of CaMKII and GSK3α/β phosphorylation in the mouse brain. **a**–**f** Western blotting analysis of p-CaMKII, CaMKII, ^{21}Ser p-GSK3α, ^{9}Ser p-GSK3β, ^{279}Tyr p-GSK3α, ^{216}Tyr p-GSK3β, and GSK3α/β in brain lysates of WT and sEH$^{-/-}$ mice ($n = 5$ in each group). **g** ELISA of relative GSK3α/β activity was collected from brain lysates of WT and sEH$^{-/-}$ mice ($n = 5$ in each group). **h** Brain lysates underwent immunoprecipitation (IP) with normal IgG or anti-sEH antibody, and precipitates were probed for CaMKII and GSK3α/β by immunoblotting (IB). Data are presented as mean ± SEM. *$p < 0.05$ vs. WT mice

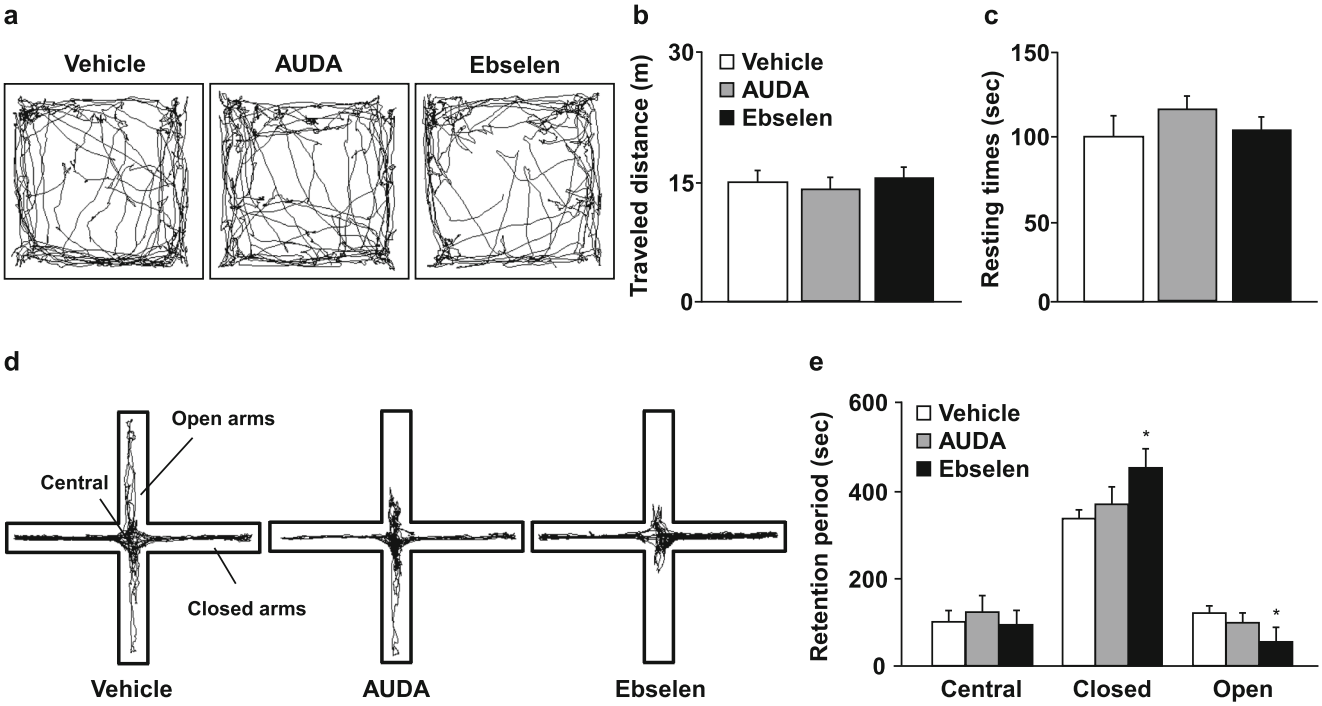

Fig. 8 sEH phosphatase activity is involved in anxiety-like behavior. **a** Representative activity traces from vehicle, AUDA, and ebselen groups of WT mice. **b**, **c** Total distance traveled and resting time of vehicle, AUDA, and ebselen groups were measured in the open field activity test. **d** Schematic diagram of EPM and representative running tracks of vehicle, AUDA, and ebselen groups. **e** The times spent in the central, closed, and open arms were measured in vehicle, AUDA, and ebselen groups of WT mice. Data are presented as mean ± SEM from 8 mice in each group. $*p < 0.05$ vs. vehicle-treated group

maintaining normal structure and physiological function. Our current findings from $sEH^{-/-}$ mice further support this argument.

It is well-established that nervous system function depends on the complex architecture of neuronal networks [30, 33, 34]. This notion is further supported by our current findings that $sEH^{-/-}$ mice exhibited better hippocampus-dependent fear-related learning and memory accompanied by reformed neurite structure of neurons in the hippocampus. Thus, in terms of branching complexity and length of neurites, deletion of sEH in mice could potentially lead to modification of circuitry and may be the cellular basis underlying altered anxiety, fear-related learning, and memory. Accordingly, these findings suggest that sEH is an important molecule that regulates diverse physiological functions of the CNS.

We investigated anxiety-related behaviors in $sEH^{-/-}$ mice using several behavior tests. In open field activity, $sEH^{-/-}$ mice demonstrated less travel distance and resting time. Notably, moving along the edges of the cage was the main exploration pattern of $sEH^{-/-}$ mice in a novel environment,

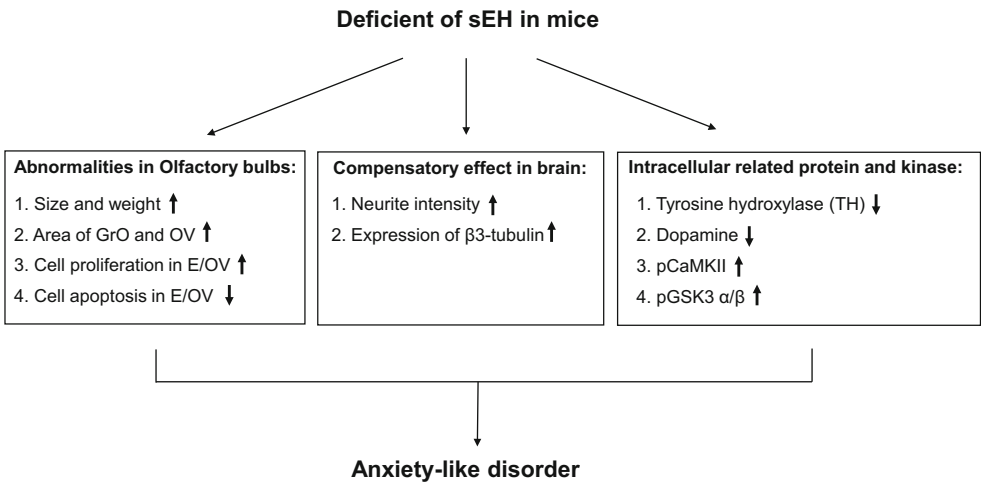

Fig. 9 Role of sEH in anxiety-like behavior in mice. A proposed mechanism of genetic deletion of sEH causes anxiety-like behavior by dysregulating OB development and dopaminergic signaling-related proteins and kinases

indicating that sEH$^{-/-}$ mice were reluctant to explore new environments in favor of resting along the corners and edges. The EPM test is an accurate method to demonstrate anxiety-like behavior in rodents [35]. We observed that sEH-deficient mice exhibited a preference for the closed arms, based on both movement pattern and retention time. Collectively, these findings suggest that sEH may play a crucial role in regulating anxiety-like behavior. Hippocampus- and amygdala-dependent fear-related learning and memory using classical fear conditioning have long been applied to investigate anxiety disorders [36]. We used tone and foot shock conditioning tests to examine anxiety-like responses in WT and sEH$^{-/-}$ mice. Compared to WT mice, sEH$^{-/-}$ mice displayed more effective learning patterns based on the degree of freezing in the fear conditioning test. Intriguingly, sEH$^{-/-}$ mice demonstrated a similar pattern of hippocampus-dependent spatial learning and memory in the MWM. WT mice demonstrated a trend to locate the platform faster than that of sEH$^{-/-}$ mice during training days in the water maze. However, there was no significant difference in the latency to find the target between sEH$^{-/-}$ and WT mice. Based on Golgi staining, sEH$^{-/-}$ mice demonstrated a compensatory effect in neurite circuitry in the hippocampus, implying that sEH deficiency may influence emotional memory rather than spatial memory. Collectively, these results suggest that the enhanced fear learning in sEH$^{-/-}$ mice seems to be more strongly associated with emotional-related processes.

The dopaminergic and serotoninergic pathway deficit hypothesis is the most widely discussed theory in anxiety disorders. This theory proposes that dopaminergic pathways negatively regulate the hippocampus-prefrontal cortex-amygdala pathway in anxiety disorders [19, 20]. The neurons of dopaminergic pathways are mainly found in areas such as the substantia nigra and striatum, which produce dopamine and transmit dopamine via projecting axons to their synaptic destinations, including the hippocampus, prefrontal cortex, and amygdala [20, 21]. Several clinical studies reported that abnormalities in dopaminergic and serotonergic systems are observed in patients with generalized social anxiety disorder [37, 38]. Our findings demonstrated that sEH$^{-/-}$ mice had a decreased level of dopamine, which was attributed to the down-regulation of TH in the substantia nigra and striatum. However, the expression of serotonin-related genes was not affected in sEH$^{-/-}$ mice compared to WT mice.

Several lines of evidence suggest that GSK3α/β plays a key role in regulating the expression of TH during development of dopaminergic neurons through transcription factor Nurr1 [39, 40]. However, whether the decreased expression of TH in dopaminergic neurons in sEH$^{-/-}$ mice is modulated by the GSK3α/β-Nurr1 pathway requires further investigation. Dysregulation of phosphorylation in CaMKII and GSK3α/β in the brain is known to play a crucial role in anxiety-like behavior [22–26]. Our data support this notion, as sEH$^{-/-}$ mice demonstrated hyperphosphorylation of CaMKII and GSK3α/β in the brain. sEH is an enzyme with EH and PT activities and regulates various physiological functions [1–3]. In particular, sEH can bind to kinases and alter their phosphorylation status by its phosphatase activity, thereby regulating kinase activity and related cellular or physiological function [41, 42]. This is further supported by our current findings that an interaction of sEH with CaMKII and GSK3α/β was observed in the brains of WT mice, which may partly explain the hyperphosphorylation of CaMKII and GSK3α/β in the brains of sEH$^{-/-}$ mice. However, Seubert et al. and Wu et al. found that genetic deletion of sEH or pharmacological inhibition of EH activity resulted in the elevation of EETs, which eventually caused hyperphopsphorylation of CaMKII or GSK3α/β [43, 44]. In this study, we could not exclude the possible involvement of EETs in the hyperphopsphorylation of CaMKII and GSK3α/β observed in sEH$^{-/-}$ mice. In spite of the unique pathway discovered in our study, further investigations are warranted to clarify the detailed molecular mechanisms by which sEH modulates the activity of CaMKII and GSK3α/β and regulates anxiety-like behavior.

To address which enzymatic activity of sEH is responsible for anxiety-like behavior in sEH$^{-/-}$ mice, we administered specific pharmacological inhibitors of EH and PT activity, namely, AUDA and ebselen, respectively. Our results revealed that inhibition of EH activity by AUDA administration did not change the pattern of behavior in open field activity or EPM compared to the vehicle group. Interestingly, inhibition of PT activity by ebselen administration increased the retention times in the closed arm of the EPM compared to the vehicle group, which was similar to the results demonstrated by sEH$^{-/-}$ mice. It has been demonstrated that certain small lipid-soluble drugs with a molecular weight < 400 Da may cross the blood-brain barrier (BBB) [45]. Both AUDA and ebselen are lipid-soluble, with molecular weights of 392.6 Da and 274.18 Da, respectively. Thus, we hypothesize that ebselen may be successfully delivered into the brain through the BBB. Nevertheless, ebselen-induced behavior changes are not as pronounced as those of sEH$^{-/-}$ mice. This may be due to the inefficiency or insufficient concentration of drugs delivered into the brain. Based on these observations, we suggest that the PT activity of sEH may play a role in the regulation of anxiety-like behavior in mice.

In conclusion, we demonstrate that sEH may interact with CaMKII and GSK3α/β, which may be pivotal for regulating neuronal differentiation, OB development, and dopamine synthesis, as well as anxiety-like behavior in mice. In this study, we provide new insights into the biological functions of sEH in the brain. Our findings highlight the potential therapeutic value of targeting sEH for treating anxiety and mood disorders.

Acknowledgments The authors thank Editage for the help with language editing (online.editage.com.tw/).

Author Contributions HT Lee, KI Lee, and HC Lin performed experiments or analyzed the data. TS Lee designed the experiments and wrote to the paper. All authors have read and approved the submission of the manuscript.

Funding Information This study was supported by grants from the Cheng-Hsin General Hospital (CY10606 and CY10708) and Ministry of Science and Technology of Taiwan (105-2320-B-010-036, 105-2811-B-010-022, 106-2320-B-002-057-MY3, 106-2320-B-002-056, and 106-2811-B-002-146).

Compliance with Ethical Standards

The experiments conformed to the Guide for the Care and Use of Laboratory Animals (Institute of Laboratory Animal Resources, eighth edition, 2011). All animal experiments were approved by the Animal Care and Utilization Committee of National Yang-Ming University.

Conflict of Interest The authors declare that they have no conflict of interest.

References

1. Gill SS, Hammock BD (2009) Distribution and properties of a mammalian soluble epoxide hydrase. Biochem Pharmacol 29: 389–395
2. Enayetallah AE, French RA, Thibodeau MS, Grant DF (2004) Distribution of soluble epoxide hydrolase and of cytochrome P450 2C8, 2C9, and 2J2 in human tissues. J Histochem Cytochem 52:447–454
3. Johansson C, Stark A, Sandberg M, Ek B, Rask L, Meijer J (1995) Tissue specific basal expression of soluble murine epoxide hydrolase and effects of clofibrate on the mRNA levels in extrahepatic tissues and liver. Arch Toxicol 70:61–63
4. Sura P, Sura R, Enayetallah AE, Grant DF (2008) Distribution and expression of soluble epoxide hydrolase in human brain. J Histochem Cytochem 56:551–559
5. Zhang W, Koerner IP, Noppens R, Grafe M, Tsai HJ, Morisseau C, Luria A, Hammock BD et al (2007) Soluble epoxide hydrolase: a novel therapeutic target in stroke. J Cereb Blood Flow Metab 27: 1931–1940
6. Wang J, Fujiyoshi T, Kosaka Y, Raybuck JD, Lattal KM, Ikeda M, Herson PS, Koerner IP (2013) Inhibition of soluble epoxide hydrolase after cardiac arrest/cardiopulmonary resuscitation induces a neuroprotective phenotype in activated microglia and improves neuronal survival. J Cereb Blood Flow Metab 33:1574–1581
7. Spector AA, Fang X, Snyder GD, Weintraub NL (2004) Epoxyeicosatrienoic acids (EETs): metabolism and biochemical function. Prog Lipid Res 2004(43):55–90
8. Inceoglu B, Jinks SL, Ulu A, Hegedus CM, Georgi K, Schmelzer KR, Wagner K, Jones PD et al (2008) Soluble epoxide hydrolase and epoxyeicosatrienoic acids modulates two distinct an algesic pathway. Proc Natl Acad Sci U S A 105:18901–18906
9. Lee J, Dahl M, Grande P, Tybjaerg-Hansen A, Nordestgaard BG (2010) Genetically reduced soluble epoxide hydrolase activity and risk of stroke and other cardiovascular disease. Stroke 41:27–33
10. Iliff JJ, Alkayed NJ (2009) Soluble epoxide hydrolase inhibition: targeting multiple mechanisms of ischemic brain injury with a single agent. Future Neurol 4:179–199
11. Wang SB, Pang XB, Zhao Y, Wang YH, Zhang L, Yang XY, Fang LH, Du GH (2012) Protection of salvianolic acid on rat brain from ischemic damage via soluble epoxide hydrolase inhibition. J Asian Nat Prod Res 14:1084–1092
12. Poli G, Corda E, Martino PA, Dall'ara P, Bareggi SR, Bondiolotti G, Iulini B, Mazza M et al (2013) Therapeutic activity of inhibition of the soluble epoxide hydrolase in a mouse model of scrapie. Life Sci 92:1145–1150
13. Wang SB, Pang XB, Gao M, Fang LH, Du GH (2013) Pinecembrin protects rats against cerebral ischemic damage through soluble epoxide hydrolase and epoxyeicosatrienoic acids. Chin J Nat Med 11: 207–213
14. Zhang W, Davis CM, Edin ML, Lee CR, Zeldin DC, Alkayed NJ (2013) Role of endothelial soluble epoxide hydrolase in cerebrovascular function and ischemic injury. PLoS One 8:e61244
15. Strauss KI, Gruzdev A, Zeldin DC (2013) Altered behavioral phenotypes in soluble epoxide hydrolase knockout mice: effects of traumatic brain injury. Prostaglandings Other Lipid Mediat 104-105:18–24
16. Lissek S, Kaczkurkin AN, Rabin S, Geraci M, Pine DS, Grillon C (2013) Generalized anxiety disorder is associated with overgeneralization of classically conditioned fear. Biol Psychiatry 75:909–915
17. Barlow DH (2000) Unraveling the mysteries of anxiety and its disorders from the perspective of emotion theory. Am Psychol 55: 1247–1263
18. Adhikari A (2014) Distributed circuits underlying anxiety. Front Behav Neurosci 8:112
19. Robinson HM, Hood SD, Bell CJ, Nutt DJ (2006) Dopamine and social anxiety disorder. Rev Bras Psiquiatr 28:263–264
20. Bodea GO, Blaess S (2015) Establishing diversity in the dopaminergic system. *FEBS Lett* 589(24 Pt A):3773–3785
21. Atanasova B, Graux J, El Hage W, Hommet C, Camus V, Belzung C (2008) Olfaction: a potential cognitive marker of psychiatric disorders. Neurosci Biobehav Rev 32:1315–1325
22. Glinka ME, Samuels BA, Diodato A, Teillon J, Feng Mei D, Shykind BM, Hen R, Fleischmann A (2012) Olfactory deficits cause anxiety-like behaviors in mice. J Neurosci 32:6718–6725
23. Hasegawa S, Furuichi T, Yoshida T, Endoh K, Kato K, Sado M, Maeda R, Kitamoto A et al (2009) Transgenic up-regulation of alpha-CaMKII in forebrain leads to increased anxiety-like behaviors and aggression. Mol Brain 2:6
24. Earl DE, Das P, Gunning WT 3rd, Tietz EI (2012) Regulation of Ca^{2+}/calmodulin-dependent protein kinase II signaling within hippocampal glutamatergic postsynapses during flurazepam withdrawal. Neural Plast 2012:405926
25. Mines MA, Yuskaitis CJ, King MK, Beurel E, Jope RS (2010) GSK3 influences social preference and anxiety-related behaviors during social interaction in a mouse model of fragile X syndrome and autism. PLoS One 5:e9706
26. Leibrock C, Ackermann TF, Hierlmeier M, Lang F, Borgwardt S, Lang UE (2013) Akt2 deficiency is associated with anxiety and depressive behavior in mice. Cell Physiol Biochem 32:766–777
27. Oguro A, Sakamoto K, Suzuki S, Imaoka S (2009) Contribution of hydrolase and phosphatase domains in soluble epoxide hydrolase to vascular endothelial growth factor expression and cell growth. Biol Pharm Bull 32:1962–1967
28. Jamain S, Radyushkin K, Hammerschmidt K, Granon S, Boretius S, Varoqueaux F, Ramanantsoa N, Gallego J et al (2008) Reduced social interaction and ultrasonic communication in a mouse model of monogenic heritable autism. Proc Natl Acad Sci U S A 105: 1710–1715
29. Adamec R, Hebert M, Blundell J, Mervis RF (2012) Dendritic morphology of amygdala and hippocampal neurons in more and less predator stress responsive rats and more and less spontaneously anxious handled controls. Behav Brain Res 226:133–146
30. Coque L, Mukherjee S, Cao JL, Spencer S, Marvin M, Falcon E, Sidor MM, Birnbaum SG et al (2011) Specific role of VTA

dopamine neuronal firing rates and morphology in the reversal of anxiety-related, but not depression-related behavior in the ClockΔ19 mouse model of mania. Neuropsychopharmacology 36:1478–1488
31. Contreras CM, Gutiérrez-García AG, Molina-Jiménez T (2013) Anterior olfactory organ removal produces anxiety-like behavior and increases spontaneous neuronal firing rate in basal amygdala. Behav Brain Res 252:101–109
32. Petreanu L, Alvarez-Buylla A (2002) Maturation and death of adult-born olfactory bulb granule neurons: role of olfaction. J Neurosci 22:6106–6113
33. Lee PC, Dodart JC, Aron L, Finley LW, Bronson RT, Haigis MC, Yankner BA, Harper JW (2013) Altered social behavior and neuronal development in mice lacking the Uba6-Use1 ubiquitin transfer system. Mol Cell 50:172–184
34. Beutler LR, Eldred KC, Quintana A, Keene CD, Rose SE, Postupna N, Montine TJ, Palmiter RD (2011) Severely impaired learning and altered neuronal morphology in mice lacking NMDA receptors in medium spiny neurons. PLoS One 6:e28168
35. Walf AA, Frye CA (2007) The use of the elevated plus maze as an assay of anxiety-related behavior in rodents. Nat Protoc 2:322–328
36. Lissek S, Powers AS, McClure EB, Phelps EA, Woldehawariat G, Grillon C, Pine DS (2005) Classical fear conditioning in the anxiety disorders: a meta-analysis. Behav Res Ther 43:1391–1424
37. van der Wee NJ, van Veen JF, Stevens H, van Vliet IM, van Rijk PP, Westenberg HG (2008) Increased serotonin and dopamine transporter binding in psychotropic medication-naive patients with generalized social anxiety disorder shown by 123I-beta-(4-iodophenyl)-tropane SPECT. J Nucl Med 49:757–763
38. Kienast T, Hariri AR, Schlagenhauf F, Wrase J, Sterzer P, Buchholz HG, Smolka MN, Gründer G et al (2008) Dopamine in amygdala gates limbic processing of aversive stimuli in humans. Nat Neurosci 11:1381–1382
39. Kim TE, Seo JS, Yang JW, Kim MW, Kausar R, Joe E, Kim BY, Lee MA (2013) Nurr1 represses tyrosine hydroxylase expression via SIRT1 in human neural stem cells. PLoS One 8:e71469
40. Kim SY, Choi KC, Chang MS, Kim MH, Kim SY, Na YS, Lee JE, Jin BK et al (2006) The dopamine D2 receptor regulates the development of dopaminergic neurons via extracellular signal-regulated kinase and Nurr1 activation. J Neurosci 26:4567–4576
41. Hou HH, Hammock BD, Su KH, Morisseau C, Kou YR, Imaoka S, Oguro A, Shyue SK et al (2012) N-terminal domain of soluble epoxide hydrolase negatively regulates the VEGF-mediated activation of endothelial nitric oxide synthase. Cardiovasc Res 93:120–129
42. Hou HH, Liao YJ, Hsiao SH, Shyue SK, Lee TS (2015) Role of phosphatase activity of soluble epoxide hydrolase in regulating simvastatin-activated endothelial nitric oxide synthase. Sci Rep 5:13524
43. Seubert JM, Sinal CJ, Graves J, DeGraff LM, Bradbury JA, Lee CR, Goralski K, Carey MA et al (2006) Role of soluble epoxide hydrolase in postischemic recovery of heart contractile function. Circ Res 99:442–450
44. Wu HF, Chen YJ, Wu SZ, Lee CW, Chen IT, Lee YC, Huang CC, Hsing CH et al (2017) Soluble epoxide hydrolase inhibitor and 14,15-epoxyeicosatrienoic acid-facilitated long-Ttrm potentiation through cAMP and CaMKII in the hippocampus. Neural Plast 2017:3467805
45. Chen H, Konofagou EE (2014) The size of blood-brain barrier opening induced by focused ultrasound is dictated by the acoustic pressure. J Cereb Blood Flow Metab 34:1197–1204